

Probability of Warm Inflation in Loop Quantum Cosmology

L. L. Graef¹ and Rudnei O. Ramos¹

¹*Departamento de Física Teórica, Universidade do Estado do Rio de Janeiro, 20550-013 Rio de Janeiro, RJ, Brazil*

Warm inflation is analyzed in the context of Loop Quantum Cosmology (LQC). The bounce in LQC provides a mean through which a Liouville measure can be defined, which has been used previously to characterize the a priori probability for inflation in LQC. Here we take advantage of the tools provided by LQC to study instead the a priori probability for warm inflation dynamics in the context of a monomial quartic inflaton potential. We study not only the question of how a general warm inflation dynamics can be realized in LQC with an appropriate number of e-folds, but also how such dynamics is constrained to be in agreement with the latest cosmic microwave background radiation from Planck. The fraction of warm inflation trajectories in LQC that gives both the required minimum amount e-folds of expansion and also passes through the observational window of allowed values for the tensor-to-scalar ratio and the spectral tilt is explicitly obtained. We find that the probability of warm inflation with a monomial quartic potential in LQC is higher than that of cold inflation in the same context. Furthermore, we also obtain that the a priori probability gets higher as the inherent dissipation of the warm inflation dynamics increases.

I. INTRODUCTION

The inflationary scenario [1] is the current paradigm for the evolution of the early universe. Inflation is able to explain several puzzles of the standard Big Bang cosmology, solving the horizon and flatness problems and explaining the origin of inhomogeneities in the universe, leading to large scale structure formation, based on causal physics. Despite of its great success, standard inflation has always been challenged by several conceptual problems since its inception. The need for a large amount of fine-tuning in the parameters of the model, the difficulties associated with the process of reheating and the problem in determining an appropriated measure with which one can determine probabilities [2], are some of the problems which has been topic of much debate [3–5]. In addition, after the Planck results [6, 7], some of the simplest inflationary models, like the monomials quadratic and quartic potentials for the inflaton field, were also disfavored by the data.

It is interesting to note that some of the aforementioned problems have been analyzed in the context of warm inflation (WI) dynamics. WI [8] differentiates itself from the usual cold inflation (CI) picture by accounting for the possible nonequilibrium dissipative processes emerging from the microscopic dynamics of the inflaton field and its necessary couplings to other particle fields degrees of freedom. It has been shown that nonequilibrium dissipation still during the slow-roll evolution of the inflaton field can be potentially strong enough to produce a quasi equilibrium thermal radiation bath during inflation. Along with the produced dissipation effect, this can strongly affect the dynamics of inflation both at the background and perturbation levels (for reviews on WI, see, e.g., Refs. [9, 10]). WI has much developed in recent years such as to be able to provide insights on some outstanding problems related to the inflationary picture and which CI cannot directly answer. Some of these insights include for example the question of eternal inflation in the context of WI [11], a solution for the so called η -problem [12]

that appears in supergravity or string inflation models, the role of dissipation in selecting favorable inflationary trajectories and in alleviating the fine-tuning problem of inflation [13, 14] (see also Ref. [15] for a recent detailed analysis of the effect of dissipation and stochastic noise effects, typical of warm inflation dynamics, in setting initial conditions for inflation). This latter point is also connected with the naturalness of inflation. It intends to address the question of whether a sufficient duration of slow-roll dynamics can occur naturally or if it requires a careful fine-tuning of initial parameters. Already in Ref. [16] it was shown that inflation can be more general in the presence of dissipation. As it is well known [17–21] WI is also able to decrease the tensor-to-scalar ratio value, rehabilitating several models ruled out in the CI context by the Planck data. In particular, recently in Ref. [22] it was analyzed how several primordial inflaton potentials can be rendered compatible with the recent Planck data in the context of WI.

In spite of all the progress made in CI and WI, neither can address one of the most important aspects of the Big Bang cosmology, the singularity problem, which is in fact a problem related to the General Relativity (GR). For any equation of state obeying the strong energy condition $p > -\rho/3$, regardless of the geometry of the universe, the scale factor in a Friedmann-Lemaître-Robertson-Walker (FLRW) metric vanishes at $t = 0$, and the matter density diverges, leading to a collapse in FLRW geometry. In fact, all the curvature invariants become singular, which is the reason why this is called the Big Bang singularity problem. However, it is common sense that in approaching the Big Bang singularity we should enter in a regime where modifications of GR are important, since ultraviolet effects are expected to become relevant in the large curvature regime. It was shown that in some scenarios these effects can smooth the Big Bang singularity. In particular, one of these scenarios, which is believed to be a possible candidate for a quantum theory of gravity, is Loop Quantum Gravity (LQG) (see, e.g., Refs. [23, 24] for some recent reviews). LQC arises as the result of ap-

plying principles of LQG to cosmological settings (see, e.g., Refs. [25–27] for recent reviews). In LQC, which is the formalism we will be focusing in this work, the quantum geometry creates a brand new repulsive force that is totally negligible at low space-time curvature but rises very rapidly in the Planck regime, overwhelming the classical gravitational attraction. In cosmological models, while Einstein’s equations hold to an excellent degree of approximation at low curvature, they undergo major modifications in the Planck regime: For matter satisfying the usual energy conditions any time a curvature invariant grows to the Planck scale, quantum geometry effects dilute it, thereby resolving singularities of GR [25, 28–30]. In addition, as shown in Refs. [31, 32], the ambiguity in defining a measure present in GR is naturally resolved in LQC because in these scenarios the Big Bang is replaced by a Big Bounce, and the bounce surface can be used to introduce the structure necessary to specify a satisfactory Liouville measure. Using this feature, the authors in Ref. [32] then makes a detailed investigation of what would be the a priori probability of a sufficiently long slow roll inflation in LQC which is compatible with the data. Taking a monomial quadratic inflaton potential as an example, they then showed that the a priori probability of having enough inflation (i.e., such that the number of e-foldings is $N_e \gtrsim 67$ as considered in Ref. [32]) is very close to one. The probability problem of inflation in LQC was also subsequently investigated in Ref. [33], while in Ref. [34] a throughout interpretation of the Liouville measure provided in LQC was given (see also Refs. [35, 36] for a different approach for determining the probability of inflation in LQC).

In the present work, we make a detailed analysis of the dynamical system of equations for inflation in LQC, including dissipative effects in the context of WI. By taking advantage of the fact that LQC provides a well defined measure with which one can compute probabilities for trajectories in phase space to have some minimum number of e-folds, we then apply that for WI. We firstly analyze the fraction of solutions in the phase space which gives the expected amount of inflation, as done in previous works in the context of CI [32, 33]. Then we go a step further and obtain also the fraction of those trajectories in WI that is consistent with the Planck data, i.e., those trajectories that cross the observational window of values for the tensor-to-scalar ratio r and the spectral tilt n_s . This is done in particular for the chaotic monomial quartic inflaton potential in the context of WI. Recall that even though LQC can predict that inflation can be quite natural with such potential, giving a probability quite close to one for obtaining at least the minimum number of e-folds needed to solve the flatness and horizon problems, the quartic potential in CI is well excluded by the Planck data [7]. Thus, even in LQC, there would be simply a vanishing probability of rendering this potential in CI compatible with the present observational data. As already mentioned, in WI the monomial quartic potential can be rendered compatible with the observations

as a consequence of dissipative effects. See in particular Refs. [18, 37] for two particular realizations in the context of WI which we will also consider in the present work. Thus, we not only access the probability of WI in LQC, but also its viability when enforcing that those inflationary trajectories should necessarily satisfy the observations. Although there have been some previous studies of WI in LQC [38–44], none of these works have focused on the questions we aim to answer in this work and, in particular, on the probability of WI in LQC. In addition, we also make use here of the most well motivated forms of the dissipative dynamics in WI, as derived by successful microscopic dynamics in nonequilibrium quantum field theory applied to WI model building.

This paper is organized as follows. In Sec. II, we briefly introduce some of the key expressions in LQC and the respective dynamics in the context of WI. Both the basic background quantities and the results for the primordial power spectrum in WI are given. In Sec. III, we give some examples of evolution in the LQC context and obtain the relevant input to be used in the computation of the probability, based on the Liouville measure introduced in Refs. [31, 32]. In Sec. IV, we compute the a priori probability of WI in LQC for different dissipation models, focusing on the cases leading to consistency with the Planck results. Finally, in Sec. V, we give our conclusions and comment on possible extensions of this work.

II. WARM INFLATION IN LQC

Let us start this section by very briefly reviewing some of the relevant results from LQC that will be useful for us. Then, we will also present some of the equations and corresponding dynamics of WI.

A. LQC dynamics

In LQC cosmological models are quantized using the methods of LQG. Below, we follow Ref. [32] in order to briefly introduce the modification of the Friedmann’s equation in LQC. The spatial geometry in LQC is encoded in the volume of a fixed, fiducial cubic cell, rather than the scale factor a , denoted by

$$v = \frac{4\mathcal{V}_0 a^3 M_{\text{Pl}}^2}{\gamma}, \quad (2.1)$$

where \mathcal{V}_0 is the comoving volume of the fiducial cell, γ is the Barbero-Immirzi parameter of LQC, whose numerical value we set as given by $\gamma \simeq 0.2375$, obtained from black hole calculations [45], and $M_{\text{Pl}} \equiv 1/\sqrt{8\pi G} = 2.4 \times 10^{18} \text{GeV}$ is the reduced Planck mass. The conjugate momentum to v is denoted by b and it is given by

$$b = -\frac{\gamma P_{(a)}}{6a^2 \mathcal{V}_0 M_{\text{Pl}}^2}, \quad (2.2)$$

where $P_{(a)}$ is the conjugate momentum to the scale factor. The variables v and b satisfy the fundamental Poisson bracket, $\{v, b\} = -2$. The equation of motion for v is given by [25]

$$\dot{v} = \frac{3v}{\gamma\lambda} \sin(\lambda b) \cos(\lambda b), \quad (2.3)$$

where λ is the constant

$$\lambda^2 = \frac{\sqrt{3}\gamma}{2M_{\text{Pl}}^2}. \quad (2.4)$$

The solution of the LQC effective equations implies that the Hubble parameter can be written as

$$H = \frac{1}{2\gamma\lambda} \sin(2\lambda b). \quad (2.5)$$

In LQC, b ranges over $(0, \pi/\lambda)$ and GR is recovered in the limit $\lambda \rightarrow 0$. The energy density ρ relates to the LQC variable b through

$$\frac{\sin^2(\lambda b)}{\gamma^2 \lambda^2} = \frac{1}{3M_{\text{Pl}}^2} \rho, \quad (2.6)$$

which combined with Eq. (2.5), leads to the Friedmann's equation in LQC,

$$\frac{1}{9} \left(\frac{\dot{v}}{v} \right)^2 \equiv H^2 = \frac{1}{3M_{\text{Pl}}^2} \rho \left(1 - \frac{\rho}{\rho_{\text{cr}}} \right), \quad (2.7)$$

where

$$\rho_{\text{cr}} = \frac{3}{\gamma^2 \lambda^2} M_{\text{Pl}}^2 = \frac{2\sqrt{3}}{\gamma^3} M_{\text{Pl}}^4. \quad (2.8)$$

We now see explicitly from Eq. (2.7) that the singularity is replaced by a (quantum) bounce when $H = 0$ and the density reaches the critical value ρ_{cr} . In particular, for $\rho \ll \rho_{\text{cr}}$ we recover GR as expected. It is important to stress that the expression (2.7) holds independently of the particular characteristics of the inflationary regime.

B. WI background dynamics

In WI it is important to account explicitly for the presence of radiation. Hence, the total energy density in Eq. (2.7) is given by

$$\rho = \frac{\dot{\phi}^2}{2} + V(\phi) + \rho_R, \quad (2.9)$$

which accounts for the presence of the radiation fluid and the scalar field (the inflaton) ϕ . In this work we are going to consider explicitly the monomial quartic potential for the inflaton

$$V(\phi) = \frac{\Lambda}{4} \left(\frac{\phi}{M_{\text{Pl}}} \right)^4, \quad (2.10)$$

where Λ/M_{Pl}^4 denotes here the (dimensionless) quartic coupling constant. The inflaton field ϕ and the radiation energy density ρ_R form a coupled system in WI dynamics, with background evolution equations given, respectively, by

$$\ddot{\phi} + 3H\dot{\phi} + \Upsilon(\phi, T)\dot{\phi} + V_{,\phi} = 0, \quad (2.11)$$

$$\dot{\rho}_R + 4H\rho_R = \Upsilon(\phi, T)\dot{\phi}^2, \quad (2.12)$$

where $\Upsilon(\phi, T)$ is the dissipation coefficient in WI, which can be a function of the temperature and/or the background inflaton field. We will define below explicitly the two cases of dissipation coefficient we will be considering in this work. For a radiation bath of relativistic particles, the radiation energy density is given by $\rho_R = \pi^2 g_* T^4/30$, where g_* is the effective number of light degrees of freedom (g_* is fixed according to the dissipation regime and interactions form used in WI).

The dissipation coefficient Υ in Eqs. (2.11) and (2.12) embodies the microscopic physics resulting from the interactions between the inflaton and the other fields that can be present and accounts for the nonequilibrium dissipative processes arising from these interactions [9, 46]. In particular, we have two relevant cases of dissipation originating from previous explicit quantum field theory model building for WI. In the first case, the inflaton is coupled to heavy intermediate fields, that are in turn coupled to light radiation fields. As the inflaton slowly moves according to its potential, it can trigger the decay of these heavy intermediate fields into the light radiation fields and generates a dissipation term for the inflaton [47]. In this case, the resulting dissipation coefficient can be well described by the expression [9, 46, 48]

$$\Upsilon_{\text{cubic}} = C_3 \frac{T^3}{\phi^2}, \quad (2.13)$$

where C_3 is a dimensionless parameter that depends on the interactions specifics. Hereafter we refer to the above Υ_{cubic} as the *cubic dissipation coefficient*. This is obtained in the so-called *low temperature* regime for WI [9, 46, 48], in which the inflaton only couples to the heavy intermediate fields, whose masses are larger than the radiation temperature and, thus, the inflaton gets decoupled from the radiation fields. Typically, to be able to generate large enough dissipation through the above mechanism, it is required in general a large number of heavy intermediate fields [48]. This then reflects in the fact that for relevant dynamics leading to WI in this case, the constant C_3 in the Eq. (2.13) is typically a very large number.

More recently, it was realized another mechanism able to lead to a successful WI regime that requires minimal field content [37]. In Ref. [37] an explicit WI model realization in particle physics was constructed. It is based on a construction used in Higgs phenomenology beyond the standard model, which uses a collective symmetry where the inflaton is a pseudo-Goldstone boson. In this case the inflaton can be directly coupled to the radiation

fields and gets protection from large thermal corrections due to the symmetries obeyed by the model. The resulting dissipative coefficient, here obtained in the so called *large temperature* regime (where the fields coupled to the inflaton are light with respect to the ambient temperature), is given simply by [37]

$$\Upsilon_{\text{linear}} = C_1 T, \quad (2.14)$$

where C_1 is again a dimensionless parameter, like C_3 in Eq. (2.13), that depends on the specific interactions of the model and that leads to Eq. (2.14) (see, e.g., Ref. [37] for details). In general we have that $C_1 \ll C_3$, reflecting the smaller field content required here as compared with the cubic form of the dissipation coefficient. Hereafter, we refer to the above equation (2.14) as the *linear dissipation coefficient*.

C. The scalar curvature power spectrum in WI

In WI not only the background dynamics gets modified, but also the primordial power spectrum can be strongly influenced by the presence of the dissipative effects and the produced radiation bath. WI at the perturbation level has been studied by many works previously (see, e.g., Refs. [49–53]). The power spectrum in WI can be written explicitly as [17]

$$\Delta_{\mathcal{R}} = \left(\frac{H_*^2}{2\pi\dot{\phi}_*} \right)^2 \left(1 + 2n_* + \frac{2\sqrt{3}\pi Q_*}{\sqrt{3+4\pi Q_*}} \frac{T_*}{H_*} \right) G(Q_*), \quad (2.15)$$

where Q_* denotes the ratio

$$Q_* = \frac{\Upsilon(T_*, \phi_*)}{3H_*}. \quad (2.16)$$

The subindex “*” indicates that the quantities are evaluated at Hubble radius crossing. The quantities in the primordial power spectrum of Eq. (2.15) are then evaluated when the relevant CMB modes cross the Hubble radius around $N_* \approx 50 - 60$ e-folds before the end of inflation. In this work we will consider $N_* = 60$ for definiteness. In Eq. (2.15), n_* denotes the inflaton statistical distribution due to the presence of the radiation bath. Here, as also in previous works (e.g., like in Ref. [22]), we will assume a thermal equilibrium distribution function $n_* \equiv n_{k_*}$ for the inflaton and, thus, it assumes the Bose-Einstein distribution form, $n_* = 1/[\exp(H_*/T_*) - 1]$. In fact, as shown recently in Ref. [54], due to the presence of the radiation bath and the inflationary dynamics itself in WI, there can always be a nonvanishing statistical distribution for the inflaton which can be close to the thermal one, even if the inflaton interaction rate with the radiation bath particles is smaller than H . The function $G(Q_*)$ in Eq. (2.15) accounts for the growth of inflaton fluctuations due to its coupling with the radiation fluid (this comes explicitly from the expression for the dissipation coefficient Υ , which in general is an explicit

function of the temperature, thus coupling both inflaton and radiation perturbations). It can only be determined numerically by solving the full set of perturbation equations found in WI [19, 37, 50, 51]. According to the method of the previous works, we use a numerical fit for $G(Q_*)$. Here we follow the notation used in Ref. [22] and we consider for the linear dissipation coefficient Υ_{linear} , that $G(Q_*)$ is given by

$$G_{\text{linear}}(Q_*) \simeq 1 + 0.335Q_*^{1.364} + 0.0185Q_*^{2.315}, \quad (2.17)$$

while for the cubic dissipation coefficient, Υ_{cubic} , $G(Q_*)$ is given by

$$G_{\text{cubic}}(Q_*) \simeq 1 + 4.981Q_*^{1.946} + 0.127Q_*^{4.330}. \quad (2.18)$$

Note that the CMB data constrains the amplitude of the scalar curvature power spectrum at a pivot scale k_* as being $\Delta_{\mathcal{R}}(k = k_*) \simeq 2.2 \times 10^{-9}$, with $k_* = 0.05 \text{ Mpc}^{-1}$, as considered by the Planck Collaboration [7]. This is the CMB normalization we use in this work.

Given the scalar curvature power spectrum expression, Eq. (2.15), the tensor-to-scalar ratio r and the spectral tilt n_s follow from their usual definitions, just like in the CI case,

$$r = \frac{\Delta_T}{\Delta_{\mathcal{R}}}, \quad (2.19)$$

and

$$n_s - 1 = \lim_{k \rightarrow k_*} \frac{d \ln \Delta_{\mathcal{R}}(k/k_*)}{d \ln(k/k_*)}, \quad (2.20)$$

where $\Delta_T = 2H_*^2/(\pi^2 M_p^2)$ is the tensor power spectrum. Due to the weakness of gravitational interactions, the tensor modes are expected not to be affected by the dissipative dynamics and Δ_T remains essentially unaltered from the CI result [17] (see also Ref. [55] for a recent study on the possible changes of the tensor spectrum in WI).

In Fig. 1 we show the results obtained for both r and n_s in WI for the two forms of dissipative coefficients given by Eqs. (2.13) and (2.14). For reference, in each dissipation case, we have indicated the values of the dissipation ratio Q_* for which we can find consistency with the Planck results. For the cubic dissipation coefficient form, we thus find that WI with the quartic inflaton potential can be rendered compatible with the Planck data for values of dissipation ratio Q_* satisfying $1.8 \times 10^{-5} \lesssim Q_* \lesssim 0.053$. For the case with the linear dissipation coefficient, even a larger range of values is allowed, given by $4.0 \times 10^{-7} \lesssim Q_* \lesssim 3.08$. Note that in CI, for the quartic potential we have that $r \simeq 0.266$ and $n_s \simeq 0.95$, thus laying well outside the allowed Planck region. WI dissipative effects effectively decreases the tensor-to-scalar ratio, making the quartic potential compatible with the data (see also Refs. [56, 57] for recent works showing the compatibility of the quartic potential in WI with the Planck data).

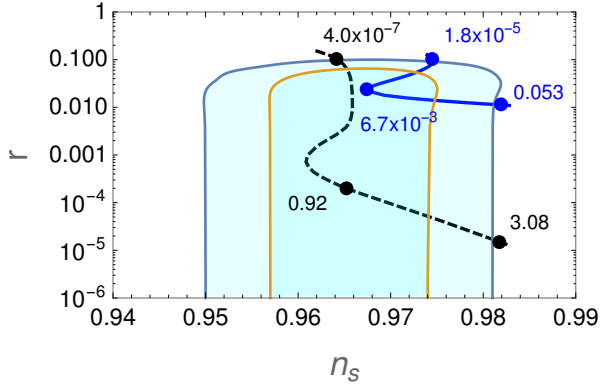


FIG. 1: The spectral index n_s and the tensor-to-scalar ratio r in the plane (n_s, r) for different values of the dissipation ratio Q_* (indicated by the numbers next to the curves), for the chaotic quartic potential. The blue solid curve shows the case of a dissipation coefficient which is cubic in the temperature while the black dashed curve shows the case of a dissipation coefficient which is linear in the temperature. The contours are for the 68% and 95% C.L. results from Planck 2015 (TT+LowP+BKP data).

D. Corrections to the power spectrum from LQC

To get the results given in the previous subsection, we have considered the dynamics as in the standard GR case, thus neglecting the LQC correction to the Friedmann's equation (2.7). This is consistent if we compare the total energy densities in the cases studied here with the critical density Eq. (2.8). For instance, for the cases shown in Fig. 1, we have that the largest energy density for the cubic dissipation case is reached for the value $Q_* = 1.8 \times 10^{-5}$. The energy density in this case is $\rho_* \equiv \rho_{\phi,*} + \rho_{R,*} \simeq 3.45 \times 10^{-9} M_{\text{Pl}}^4$. For the linear dissipation case this happens at $Q_* = 4.0 \times 10^{-7}$, with an energy density $\rho_* \simeq 3.39 \times 10^{-9} M_{\text{Pl}}^4$. Hence, in both cases we have that $\rho_* \ll \rho_{\text{cr}} \simeq 258.58 M_{\text{Pl}}^4$ and quantum effects on the geometry from LQC can be neglected in principle. However, even though at the background level this can be certain, we have to evaluate with care the LQC contributions at the perturbation level. In particular, the power spectrum can receive important contributions due to LQC, including even the presence of features, as recent works have shown.

In the cold inflationary scenarios in GR, it is assumed that the pre-inflationary dynamics does not have any effect on modes that are observable in the CMB. In these scenarios, these modes have physical wavelengths smaller than the curvature radius at the onset of inflation and all the way back to the Big Bang. Modes with such wavelengths do not feel the effects of the curvature, and then propagates as if they were in flat spacetime, with a trivial dynamics. However, the situation is different in LQC due to the distinct pre-inflationary dynamics. In this scenario some of the relevant modes have physical wavelengths comparable to the curvature radius at the bounce time.

As showed by Parker [58], modes that experience curvature are excited. So, large wavelength modes are excited in the Planck regime that follows the bounce. As a consequence, at the onset of inflation, the quantum state of perturbations is populated by excitations of these modes over the Bunch-Davis vacuum, changing the initial conditions for perturbations at the onset of inflation [59]. Due to this, the scalar curvature power spectrum in LQC gets modified with respect to GR, such that it can be written as¹

$$\Delta_{\mathcal{R}}(k) = |\alpha_k + \beta_k|^2 \Delta_{\mathcal{R}}^{GR}(k), \quad (2.21)$$

where α_k and β_k are the Bogoliubov coefficients, where the pre-inflationary effects are codified and $\Delta_{\mathcal{R}}^{GR}$ is the GR form for the power spectrum, e.g., given by Eq. (2.15). Below, we follow, in particular, the derivation done recently in Ref. [60].

Equation (2.21) can be parametrized as

$$\Delta_{\mathcal{R}}(k) = (1 + \delta_{PL}) \Delta_{\mathcal{R}}^{GR}(k). \quad (2.22)$$

The factor δ_{PL} in the above equation is k -dependent and it takes into account the LQC corrections. It is given by [60]

$$\begin{aligned} \delta_{PL} = & \left[1 + \cos\left(\frac{\pi}{\sqrt{3}}\right) \right] \text{csch}^2\left(\frac{\pi k}{\sqrt{6}k_B}\right) \\ & + \sqrt{2} \sqrt{\cosh\left(\frac{2\pi k}{\sqrt{6}k_B}\right) + \cos\left(\frac{\pi}{\sqrt{3}}\right)} \cos\left(\frac{\pi}{2\sqrt{3}}\right) \\ & \times \text{csch}^2\left(\frac{\pi k}{\sqrt{6}k_B}\right) \cos(2k\eta_B + \varphi_k), \end{aligned} \quad (2.23)$$

where φ_k is given by

$$\varphi_k \equiv \arctan \left\{ \frac{\text{Im}[\Gamma(a_1)\Gamma(a_2)\Gamma^2(a_3 - a_1 - a_2)]}{\text{Re}[\Gamma(a_1)\Gamma(a_2)\Gamma^2(a_3 - a_1 - a_2)]} \right\}, \quad (2.24)$$

where the a_1, a_2, a_3 are defined as $a_{1,2} = (1 \pm 1/\sqrt{3})/2 - ik/(\sqrt{6}k_B)$ and $a_3 = 1 - ik/(\sqrt{6}k_B)$ and the index B in the quantities in the above equations indicates that they are calculated at the bounce. In particular, η_B is the conformal time at the bounce and $k_B = \sqrt{\rho_{\text{cr}}} a_B / M_{\text{Pl}}$ is a characteristic scale at the bounce.

The term in Eq. (2.23) with $\cos(2k\eta_B + \varphi_k)$ oscillates very fast and has negligible effect when averaging out in time. The factor δ_{PL} then simplifies to

$$\delta_{PL} = \left[1 + \cos\left(\frac{\pi}{\sqrt{3}}\right) \right] \text{csch}^2\left(\frac{\pi k}{\sqrt{6}k_B}\right). \quad (2.25)$$

Since this pre-factor represents the effects of the pre-inflationary dynamics, it has the same expression in both the cold and warm inflationary pictures.

¹ Here, we will follow the notation of Ref. [60], where a complete derivation of these pre-inflationary LQC modifications to the GR spectrum were given.

Likewise, the tensor spectrum in the LQC can be written as [60]

$$\Delta_T(k) = (1 + \delta_{PL})\Delta_T^{GR}(k), \quad (2.26)$$

where $\Delta_T^{GR}(k)$ is the tensor spectrum in standard CI. As already explained in the previous subsection, due to the weakness of gravitational interactions, $\Delta_T^{GR}(k)$ in WI has basically the same expression as in CI. It is remarkable to note that the pre-factor δ_{PL} for both scalar and tensor perturbations are equal, and are given by Eq. (2.25). As a result, the tensor-to-scalar ratio is the same as that given in GR.

As discussed by the authors of Ref. [60], in standard inflation, in addition to the usual number of e-folds $N_* \equiv \ln(a_{end}/a_*) \approx 60$ required in general, it is necessary an extra amount of expansion $\delta N \equiv \ln(a_*/a_B) \gtrsim 21$, in order for the model to be consistent with observations. As shown in Ref. [60], after the effects of the pre-inflationary dynamics are taken into account, the power spectra are generically scale-dependent and exhibits oscillatory features (note that oscillatory features in the power spectrum in bouncing models is a generic result, as shown, e.g., recently in Ref. [61]). As a consequence, in order to be consistent with observations, the universe must have expanded at least 21 e-folds from the bounce till Hubble radius crossing at the observables scales, such as to allow for these scale-dependent features to get sufficiently diluted away and not spoiling the perturbation spectra of CMB. This is why, in the analysis that will follow below, in addition of the usual minimum 60 e-folds of inflation (referring to the amount of expansion from Hubble radius crossing N_* to the end of inflation), we will also consider at least 21 additional e-folds from the bouncing time till N_* . Therefore, we will consider a total of at least 81 e-folds from the bounce till the end of inflation, such that any pre-inflationary effects are sufficiently diluted and do not spoil the observed spectrum (see also Ref. [62] and references therein for a discussion about these and other LQC effects).

III. ILLUSTRATION OF THE DYNAMICS IN LQC FOR THE CI AND WI PICTURES

A. The phase space system

It is always useful to look the background dynamics as a dynamical system. In this way, the inflaton's equation of motion, Eq. (2.11), together with $\dot{\phi} = d\phi/dt$ and the time derivative for the Hubble parameter,

$$\dot{H} = -\frac{1}{2M_{\text{Pl}}^2} \left(\dot{\phi}^2 + \frac{4}{3}\rho_R \right) \left[1 - \frac{\dot{\phi}^2 + 2V(\phi) + 2\rho_R}{\rho_{\text{cr}}} \right], \quad (3.1)$$

form a three-dimensional (dissipative) dynamical system² in the phase space $(\phi, \dot{\phi}, H)$. Since the radiation energy density satisfies $\rho_R \geq 0$ by definition, we thus have, from Eq. (2.7), that $\phi, \dot{\phi}$ and H satisfy the inequality

$$H^2 \geq \frac{1}{3M_{\text{Pl}}^2} \left[\frac{\dot{\phi}^2}{2} + V(\phi) \right] \left[1 - \frac{\frac{\dot{\phi}^2}{2} + V(\phi)}{\rho_{\text{cr}}} \right]. \quad (3.2)$$

Hence, it defines a volume in the phase space $(\phi, \dot{\phi}, H)$ such that the physical region $\rho_R \geq 0$ is inside this volume. In LQC, the upper half of this volume, $H \geq 0$, corresponds to those trajectories that evolve from the bounce time to the future. In the absence of radiation, $\rho_R = 0$, the equality in Eq. (3.2) represents a surface, or more particularly in the language of dynamical systems, an *invariant manifold*. As a consequence, all initial conditions chosen on this surface will produce trajectories that evolve on it and end towards the origin. While for the dissipative system, in which $\rho_R \neq 0$, all trajectories with initial conditions taken inside this volume, they will evolve inside the volume of the invariant manifold. Trajectories with initial conditions taken externally to the invariant manifold, will evolve towards it, being this region then an attractor in phase space. The inflationary region in this phase space is defined by the condition,

$$\frac{\ddot{a}}{a} = \dot{H} + H^2 > 0. \quad (3.3)$$

In Fig. 2 we show an example of phase space volume in LQC for the case of the quartic potential, Eq. (2.10), with a fixed value of coupling constant $\Lambda/M_{\text{Pl}}^4 \simeq 1.51 \times 10^{-13}$. For comparison, we also show the corresponding volume in the GR case. Note that in LQC, H is naturally bounded from above, $H_{\text{max}} = 1/(2\gamma\lambda)$, as seen explicitly from Eq. (2.5), while, of course, there is no such upper bound in GR. In Fig. 2 we have truncated H in the GR case at the same value of H_{max} in LQC for illustration. The two regions coincide when $\rho \ll \rho_{\text{cr}}$, but they depart from each other as we approach the critical density value ρ_{cr} . The bounce points (shown by the horizontal dashed curve) in the phase space are clear in Fig. 2. The invariant manifold is always given by the external surface of the volumes in Fig. 2. The black line in Fig. 2 shows an example of trajectory in the phase space in the CI case, for the quartic coupling value given above, evolving from the bounce (with kinetic energy dominated initial conditions) forward in time. We can see that the Hubble parameter starts from $H = 0$ at the bounce and then increases until it reaches its maximum value, when it starts decreasing again, reaching a small positive value. Since it

² Note that ρ_R can be expressed in terms of $\phi, \dot{\phi}$ and H from the equation for the Hubble parameter, Eq. (2.7), and, hence, can be considered as the first integral of Eq. (2.12). Thus, there is no need to consider ρ_R as part of the dynamical system.

is a case in the absence of dissipation (CI), the trajectory evolves on the invariant manifold.

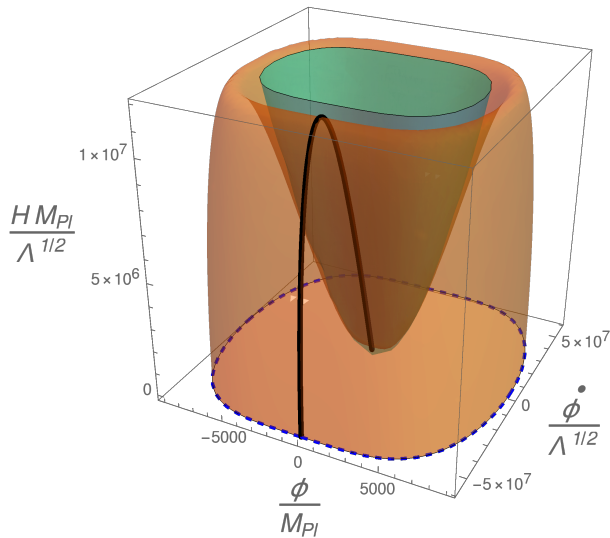


FIG. 2: The phase space available in the cases of LQC (external orange region) and in GR (internal green region). The black curve shows an example of a trajectory evolving from the bounce forward in time. The horizontal dashed curve indicates the location of the bounce, in the plane $(\phi, \dot{\phi})$.

B. Dynamics of WI in LQC

Let us now expose some of the explicit results concerning the dynamics evolution of WI in LQC. As already discussed in Sec. I, our interest is in investigating those cases for which the inflationary trajectories will cross the favorable Planck region for the observables r and n_s . Therefore, we focus on the results leading to those trajectories shown in Fig. 1. Each of the indicated dissipative points shown in Fig. 1 can be regarded as a different model, whose more fundamental origin can be seen as coming from some explicit model building for WI, which we have discussed in Sec. II B (but whose detailed particle physics specifics we will not be concerned here). Thus, we specify six cases we are going to analyze, corresponding to the points shown in Fig. 1: (a) two initial conditions leading to trajectories passing at the top extrema of the 2σ CL of the Planck contour, corresponding to the lowest values of the dissipation (one for each of the two dissipation cases given previously); (b) two initial conditions (again, one for each dissipation coefficient form) leading to trajectories passing at the center values of (r, n_s) in the Planck contour; and finally, (c) two initial conditions leading to trajectories leaving the right extremum of the 2σ CL of the Planck contour (corresponding to the cases with the largest values of dissipation coefficient consistent with the observational data).

Our numerical strategy is the following: First, the values of the field, its time derivative and the radiation energy density are obtained in each of these cases, i.e., the values of $\phi_* \equiv \phi(N_* = 60)$, $\dot{\phi}_* \equiv \dot{\phi}(N_* = 60)$ and $\rho_{R,*} \equiv \rho_R(N_* = 60)$; Then, we extrapolate the dynamics backwards in time up to the bounce time (which from now on is assumed to be our initial time, with $N_e = 0$) and obtain the respective values of the field, its time derivative and the radiation energy density at the bounce in each case, ϕ_B , $\dot{\phi}_B$ and $\rho_{R,B}$. By doing this we are certain that the evolution from this instant forward in time will lead to trajectories passing through each of the points shown in Fig. 1. As already mentioned, we focus on the cases in which from the bounce initial time till the inflationary region (with Hubble radius exit at $N_* = 60$), there is at least 21 additional e-folds of evolution, such as to allow enough time to dilute the effects discussed in Sec. II D. In addition, we will focus essentially in the case of a kinetic energy dominated bounce, i.e., $\rho_B \sim \rho_{\dot{\phi},B} \equiv \dot{\phi}_B^2/2 \sim \rho_{cr}$, with a negligible initial radiation energy density³. Thus, at the bounce, we always have $\rho_{\dot{\phi},B} \gg V(\phi_B) \gg \rho_{R,B}$. We make this choice since this is expected to be the most relevant case concerning the conditions emerging from the bounce (see, e.g., Refs. [31, 32]). A bounce dominated by the potential energy of the inflaton will always lead to extremely large number of e-folds of inflation (thus inflation is certain). In the case of a radiation energy dominated bounce, besides not being a common assumption in bouncing models (see, however, Ref. [63]), it also prevents inflation in general, except in those cases in which the inflaton potential energy density is large enough such that, as the radiation energy density dilutes faster, $V(\phi)$ can come to dominate at some point and leading to inflation (see, e.g., Ref. [15] for a discussion of the initial condition problem for inflation in this context). Since this later case is rather model dependent, we avoid addressing such situation here.

The relevant values of parameters following from the above described strategy are given in Tab. I. Since all previous results in CI have focused essentially in the monomial quadratic potential, for completeness we also give the results of CI for the quartic potential, which will be useful for future comparison with WI. In Tab. I we give the results for different inflaton coupling constants Λ/M_{Pl}^4 for each of the cases studied. These values enforce that the amplitude of the primordial scalar power spectrum is normalized with the Planck CMB results, i.e., $\Delta_{\mathcal{R}}(k = k_*) \simeq 2.2 \times 10^{-9}$. The values of the dissipation coefficient Q refers to those given in Fig. 1. The values of ϕ_{min} and ϕ_{max} give the range of initial values of in-

³ Note that here we assume that the radiation is produced by the inflaton dynamics from the bounce instant onwards. We are also not concerned in this work with any possible dynamics that might be present prior to the bounce, i.e., in the contracting phase of the universe.

TABLE I: The values of parameters used to compute the probabilities.

Case	Υ	Q_*	C_i	Λ/M_{Pl}^4	ϕ_B/M_{Pl}	$\phi_{\text{min}}/M_{\text{Pl}}$	$\phi_{\text{max}}/M_{\text{Pl}}$
CI	-	-	-	1.5115×10^{-13}	± 9095.1571	-34.3917	13.9391
WI	$\propto \frac{T^3}{\phi^2}$	1.8×10^{-5}	4.4772×10^6	9.7785×10^{-14}	± 10141.3811	-21.6089	21.6089
		6.7×10^{-3}	1.1975×10^7	5.7204×10^{-14}	± 11595.9834	-18.3440	18.3440
		0.053	1.6377×10^7	4.6832×10^{-14}	± 12190.7109	-16.6455	16.6455
WI	$\propto T$	4.0×10^{-7}	1.1561×10^{-6}	5.5389×10^{-14}	± 11689.8322	-35.8902	13.4930
		0.92	0.0121	1.6506×10^{-15}	± 28135.362	-22.1514	5.5982
		3.08	0.0181	8.0446×10^{-16}	± 33673.5327	-16.9156	1.4951

flaton amplitude for which we have less than $N_e \simeq 81$ e-folds of expansion from the bounce till the end of inflation, i.e., for field values satisfying $\phi_{\text{min}} \lesssim \phi \lesssim \phi_{\text{max}}$, we have $N_e \lesssim 81$ e-folds of expansion. The values of ϕ_B given in Tab. I are the maximum allowed initial values of the inflaton field, which correspond to the cases of a bounce dominated by the potential energy $V(\phi)$. These values are used in the definition of the probability that we are going to compute in the next section following the method given by the authors in Refs. [31, 32].

In Figs. 3 and 4 we illustrate the dynamics of WI and we also contrast it with the case of CI. For convenience, in the WI case, we use the models for which the dissipation coefficients correspond to the central values in Fig. 1, i.e., for $Q_* = 6.7 \times 10^{-3}$ in the cubic dissipation coefficient case and for $Q_* = 0.92$ in the linear dissipation one.

In Fig. 3 it is shown the evolution of each of the energy density components, i.e., the potential energy density $V(\phi)$, the kinetic energy density $\dot{\phi}^2/2$ and the radiation energy density ρ_R . As already clarified before, our initial conditions at the bounce (where we set $N_e = 0$ in the numerical calculations) always start with a kinetic energy dominated regime, with $\dot{\phi}_B^2/2 \gg V(\phi_B) \gg \rho_{R,B}$. Notice that this refers to a stiff like matter initial evolution (with equation of state $w = 1$). The kinetic energy quickly dilutes away, since $\rho_{\dot{\phi}} \propto 1/a^6$. Then, around $N_e \sim 5$, the potential energy density starts to dominate and the inflationary regime starts. Note that in the CI case, shown in the panel (a) in Fig. 3, inflation ends when the kinetic energy tends to the potential energy value and the usual (p)reheating phase can follow subsequently. The situation is different in the two WI cases. As shown in the panels (b) and (c) in Fig. 3, inflation tends to end now when the inflaton potential energy density reaches an equality with the radiation energy density produced by the dissipative process in WI. As it is typical in WI, inflation ends entering smoothly into the radiation dominated regime, without a subsequent (p)reheating phase a priori. In the two panels for the WI examples, we also see that immediately after the bounce, the radiation density is still very small relative to the potential energy.

This phase actually corresponds to a superinflation phase (happening also in the CI case), which is a typical behavior seen for LQC in the presence of scalar fields (see, e.g., Refs. [31, 32]). This super inflation regime starts right after the bounce, when $H = 0$ and lasts till H reaches its maximum values ($\dot{H} = 0$).

Note also that in the WI case, the fast evolution of the inflaton field also triggers a large radiation production through the dissipative term. The radiation energy density now raises above the potential energy and this coincides with the end of the superinflation. From this point on, the system behaves as radiation dominated and the radiation energy density decreases as $\rho_R \propto 1/a^4$ and faster than the potential energy density, till the latter dominates (at around $N_e \sim 8$ in the two WI cases shown) and the regular inflationary regime starts.

The evolution behavior in the three regimes: superinflation immediately following the bounce, a noinflationary regime and the inflationary regime, can also be seen explicitly in Fig. 4, where we show the slow-roll coefficient

$$\epsilon_H = -\frac{\dot{H}}{H^2}, \quad (3.4)$$

an instant after the bounce. It can be clearly seen in all three panels of Fig. 4 that we have a very short superinflation accelerated phase (with $\epsilon_H < 0$) lasting a fraction of an e-fold, which, after a very short transient phase, it is followed by a regular non-accelerated evolution (with $\epsilon_H > 1$) that lasts around 4 to 8 e-folds. This phase is then followed by the regular inflationary phase lasting around the remaining 73 to 77 or so e-folds.

IV. PROBABILITY OF WI IN LQC

The equation of motion for the volume variable $v(t)$ of LQC (defined by Eq. (2.1)) and for the inflaton $\phi(t)$ can be written in WI as

$$\ddot{v} = \frac{3v}{M_{\text{Pl}}^2} \left[\rho \left(1 - \frac{\rho}{\rho_{\text{cr}}} \right) - \frac{1}{2} \left(1 - 2 \frac{\rho}{\rho_{\text{cr}}} \right) \left(\dot{\phi}^2 + \frac{4}{3} \rho_R \right) \right], \quad (4.1)$$

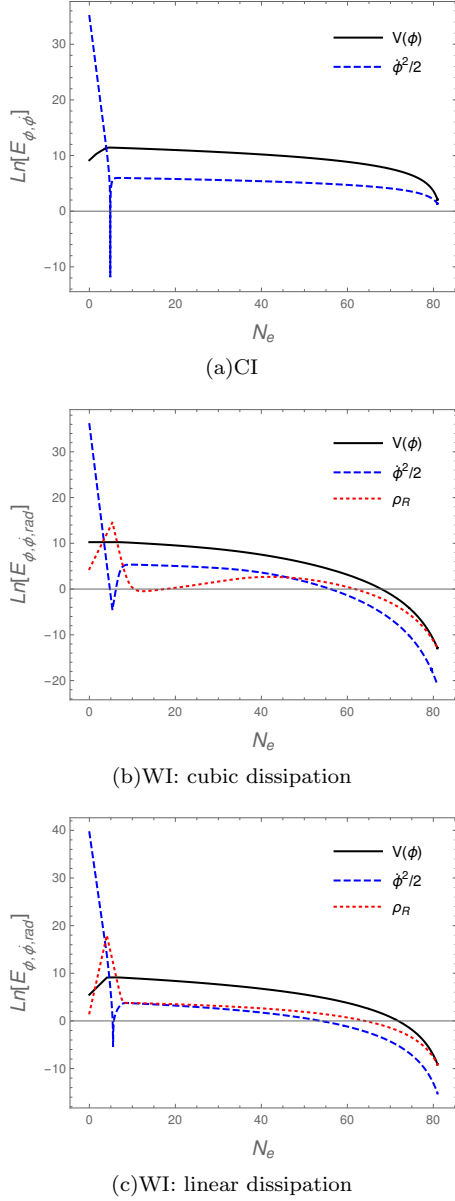


FIG. 3: The evolution (in terms of number of e-folds N_e), from the bounce till the end of inflation, for the kinetic, potential and radiation energy densities. In the vertical axis, we have the natural logarithm of the energies densities, with $E_i = V(\phi)/\Lambda, \dot{\phi}^2/(2\Lambda), \rho_R/\Lambda$ denoting the dimensionless energy density components.

and

$$\ddot{\phi} + \frac{\dot{v}}{v}\dot{\phi} + \Upsilon\dot{\phi} + V_{,\phi} = 0, \quad (4.2)$$

with $\rho \equiv \dot{\phi}^2/2 + V(\phi) + \rho_R$ in Eq. (4.1).

Here we will follow closely the procedure of Ref. [32] in their definition of the Liouville measure used in the definition of the a priori probability of inflation and extend it to WI. Let us denote the phase space as Γ . It consists of quadruplets $(v, b; \phi, p_\phi)$, with $\lambda b \in [0, \pi/2]$

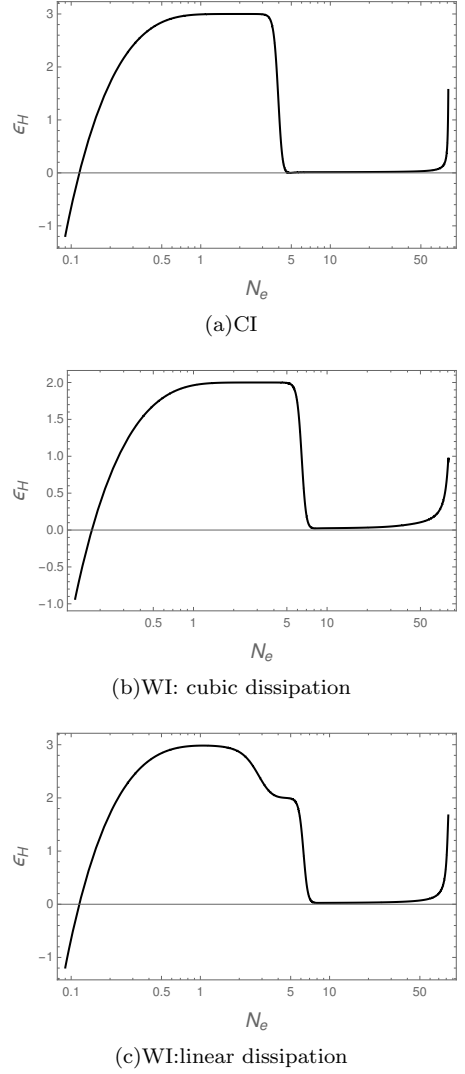


FIG. 4: The evolution (in terms of number of e-folds N_e), from an instant following the bounce till the end of inflation, for the slow-roll coefficient ϵ_H .

and $p_\phi = 2\pi\gamma l_{\text{Pl}}^2 v \dot{\phi}$, where $l_{\text{Pl}} \equiv 1/(\sqrt{8\pi}M_{\text{Pl}})$ is the Planck length. The Liouville measure on Γ is simply $d\mu_L = dv db d\phi dp_\phi$. The LQC Friedmann equation implies that these variables must lie on a constraint surface $\bar{\Gamma}$ defined by

$$\frac{3\pi}{2\lambda^2} \sin^2 \lambda b = 8\pi M_{\text{Pl}}^2 \frac{p_\phi^2}{2v^2} + \frac{\pi\gamma^2}{2M_{\text{Pl}}^2} [V(\phi) + \rho_R]. \quad (4.3)$$

The variables $(v, b; \phi, p_\phi)$ evolve via the system of coupled

equations,

$$\dot{v} = \frac{3v \sin 2\lambda b}{2\gamma \lambda}, \quad (4.4)$$

$$\dot{b} = -8M_{Pl}^2 \frac{p_\phi^2}{\gamma v^2}, \quad (4.5)$$

$$\dot{\phi} = 4M_{Pl}^2 \frac{p_\phi}{\gamma v}, \quad (4.6)$$

$$\dot{p}_\phi = -\frac{\gamma|v|}{4M_{Pl}^2} (V_\phi + \Upsilon \dot{\phi}), \quad (4.7)$$

$$\dot{\rho}_R = -\frac{4}{3} \frac{\dot{v}}{v} \rho_R + \Upsilon \dot{\phi}^2. \quad (4.8)$$

We can see that the production of radiation during inflation implies in an additional term in the expression of \dot{p}_ϕ .

By using the above equations we can analyze which fraction of all possible initial conditions evolves to an inflationary stage with the expected amount of slow-roll expansion. This will give us the probability that a sufficient amount of inflation occurs, which will provide us with means to address the question of the naturalness of inflation in the more general context of a dissipative system. Below we will then compute this probability for the two models of WI discussed in the previous sections and for each of the values of dissipation coefficient ratio (models) given in Tab. I.

In order to compute the probability of WI in LQC we need to obtain the Liouville measure on the space S of solutions to the equations of motion (4.1) and (4.2). This space of solutions S is found to be isomorphic to a gauge fixed surface, a surface $\hat{\Gamma}$ of $\bar{\Gamma}$ which is intersected by each dynamical trajectory only once [32]. Since the LQC variable b is monotonic along dynamical trajectories, we can choose $b = b_0$ (where b_0 is a fixed constant) within $\bar{\Gamma}$. The Liouville measure $d\hat{\mu}_L$ on S is independent of the choice of b_0 . The most natural choice in LQC is to set $b_0 = \pi/2\lambda$, the 'bounce surface'. The induced measure on S , $d\hat{\mu}_L = (p_\phi/v)d\phi dv$ can then be written, using Eq. (4.3), as,

$$d\hat{\mu} = \frac{1}{\sqrt{8\pi}M_{Pl}} \left\{ \frac{3\pi}{\lambda^2} \sin^2(\lambda b_0) - \frac{\pi\gamma^2}{M_{Pl}^2} [V(\phi) + \rho_R] \right\}^{1/2} d\phi dv. \quad (4.9)$$

Now, if $(\phi(t), v(t))$ is a solution to the equations of the system and let α be some constant, then $(\phi(t), \alpha v(t))$ is also a solution, since the rescaling by a constant corresponds to a rescaling of spatial coordinates (or of the fiducial cell) under which physics does not change. Therefore, this transformation corresponds to a gauge motion [32]. When computing the probabilities we can fix $v = v_0$ in the integrals and we can define the volume v_0 at the bounce to be 1. v_0 rescales the measure by a constant and therefore drops out in the calculations of probabilities. In conclusion, we made two gauge choices, $b = b_0$ and $v = v_0$.

TABLE II: The probabilities for each of the models represented by the points shown in Fig. 1. The value for CI is also shown for comparison.

Case	Υ	Q_*	$P(E_{N_e > 81})$
CI	-	-	0.99696
WI	$\propto \frac{T^3}{\phi^2}$	1.8×10^{-5}	0.99756
		6.7×10^{-3}	0.99819
		0.053	0.998438
WI	$\propto T$	4.0×10^{-7}	0.99758
		0.92	0.99944
		3.08	0.99969

The probability of occurrence of an event E can then be written as the fractional volume of the region $R(E)$ in S associated with the solutions in which E occurs. We can define this probability as

$$P(E) = \frac{\int_{R(E)} d\hat{\mu}_L}{\int_S d\hat{\mu}_L}. \quad (4.10)$$

Therefore, we can consider our gauge choices in Eq. (4.9) in order to write the probability for the occurrence of a determined amount of slow-roll inflation as [32]

$$P(E) = \frac{1}{N} \int_{I(E)} \sqrt{\frac{\gamma^2 \rho_{cr}}{8M_{Pl}^6}} \left[1 - \frac{V(\phi) + \rho_R}{\rho_{cr}} \right]^{1/2} d\phi, \quad (4.11)$$

where we have used Eq. (2.8) and in the integration sign of the above equation $I(E)$ indicates that the integral limits correspond to the limits on ϕ that generates the determined amount of slow roll inflation. The normalization N in Eq. (4.11) is given by

$$N = \int_{-\phi_B}^{+\phi_B} \sqrt{\frac{\gamma^2 \rho_{cr}}{8M_{Pl}^6}} \left[1 - \frac{V(\phi) + \rho_R}{\rho_{cr}} \right]^{1/2} d\phi. \quad (4.12)$$

Unlike the integral limits in Eq. (4.11), in the expression for N the integral covers the whole range of possible initial values for the variable ϕ . The quantities in the above expressions are evaluated at the bounce.

For simplicity, firstly we are going to compute the probability for the occurrence of less than 81 e-folds of expansion from the bounce until the end of inflation, $P_{N_e \leq 81}$. The values ϕ_{\max} and ϕ_{\min} , given explicitly in Tab. I, correspond to the maximum and minimum values, respectively, for the inflaton that gives less than 81 e-folds of expansion. After computing $P_{N_e \leq 81}$, the probability for occurrence of the expected amount of expansion (i.e., more than 81 e-folds until the end of inflation) can be easily obtained as $P_{N_e > 81} = 1 - P_{N_e \leq 81}$. In terms of the quartic potential for the inflaton, Eq. (2.10), we have that the probability $P_{N_e \leq 81}$ can be explicitly expressed as

$$P_{N_e \leq 81} = \frac{\int_{\phi_{\min}}^{\phi_{\max}} \sqrt{1 - \frac{\sqrt{3}\gamma^3}{6} \frac{\Lambda}{M_{\text{Pl}}^4} \left[\frac{1}{4} \left(\frac{\phi}{M_{\text{Pl}}} \right)^4 + \frac{\rho_R}{\Lambda} \right]} d\phi}{\int_{-\phi_B}^{+\phi_B} \sqrt{1 - \frac{\sqrt{3}\gamma^3}{6} \frac{\Lambda}{M_{\text{Pl}}^4} \left[\frac{1}{4} \left(\frac{\phi}{M_{\text{Pl}}} \right)^4 + \frac{\rho_R}{\Lambda} \right]} d\phi}. \quad (4.13)$$

Using the values given in Tab. I, the computation of the quantity $P_{N_e > 81} = 1 - P_{N_e \leq 81}$ is straightforward. Table II shows the results for the probability $P_{N_e > 81}$ of occurrence of the expected amount of inflation for all the inflationary models, represented by the points shown in Fig. 1. We can see that the probability is always very close to one in all the cases analyzed. We observe that the probability for the occurrence of a sufficient amount of WI is larger (although slightly) than the one for CI. We also see that in each of the WI models considered, the probability tends to increase with the dissipation. This can be interpreted by the fact that in the presence of dissipation, the trajectories are attracted faster to the inflationary region and they stay longer there [13, 16]. Thus, the probability tends always to be larger in WI than in CI.

V. CONCLUSIONS

In this work we have considered the warm inflationary scenario in the context of LQC. We have analyzed the modifications in the dynamical system due to quantum effects on the geometry from LQC, which produces a bounce in the place of the singularity of GR. The presence of the bounce sets the appropriate conditions where a Liouville measure can be defined properly and probabilities be computed. We have then taken advantage of this to extend previous analysis of the a priori probability in the CI picture to the case of WI. We have focused our analysis for the case of a monomial quartic potential for the inflaton, which despite being excluded in the CI case, it is not in WI. We have then obtained the appropriate conditions for which the consistency with the Planck data is assured. From these, we were able to

determine the initial conditions set at the bounce which would lead to trajectories in the phase space exactly passing through the allowed Planck region in the (r, n_s) plane. Our results have demonstrate that in WI we have a superinflation phase, as expected in general, followed by a noninflationary radiation dominated region, followed then by the usual slow-roll inflationary region, lasting long enough. In the examples given, we have also shown that this inflationary region can end smoothly in a radiation dominated regime, as is expected in general in WI.

Our results for the probability for the occurrence of at least 81 e-folds of inflation in the WI models were all consistently higher than in the CI picture. Furthermore, with the monomial quartic inflaton potential used and for the different dissipation coefficients considered, these favorable trajectories are all consistent with the Planck data. This is opposite to what happens in the CI case. In CI, despite the probability of trajectories with enough e-folds of inflation is highly probable, none of them is able to satisfy the observations.

It would be interesting, as a future work, to also study other different inflationary potentials for WI in the LQC context. In addition, a close connection with model building in WI, in the lines of e.g. Ref. [37], would also help to access these probabilities in terms of the microscopic parameters (i.e., the couplings and energy scales) of the model. This could help in constraining further these parameters and helping in the model building for WI.

Acknowledgments

L.L.G. is supported by a posdoc grant "Pós-Doutorado Nota 10" from Fundação Carlos Chagas Filho de Amparo à Pesquisa do Estado do Rio de Janeiro (FAPERJ), No. E - 26/202.511/2017. R.O.R. is partially supported by research grants from Conselho Nacional de Desenvolvimento Científico e Tecnológico (CNPq), grant No. 302545/2017-4 and Fundação Carlos Chagas Filho de Amparo à Pesquisa do Estado do Rio de Janeiro (FAPERJ), grant No. E - 26/202.892/2017.

[1] A. A. Starobinsky, *A New Type of Isotropic Cosmological Models Without Singularity*, Phys. Lett. B **91**, 99 (1980); K. Sato, *First Order Phase Transition of a Vacuum and Expansion of the Universe*, Mon. Not. Roy. Astron. Soc. **195**, 467 (1981); A. H. Guth, *The Inflationary Universe: A Possible Solution to the Horizon and Flatness Problems*, Phys. Rev. D **23**, 347 (1981); A. Albrecht, P. J. Steinhardt, *Cosmology for Grand Unified Theories with Radiatively Induced Symmetry Breaking*, Phys. Rev. Lett. **48**, 1220 (1982); A. D. Linde, *A New Inflationary Universe Scenario: A Possible Solution of the Horizon, Flatness, Homogeneity, Isotropy and Primor-*

dial Monopole Problems, Phys. Lett. B **108**, 389 (1982).
[2] G. W. Gibbons and N. Turok, *The Measure Problem in Cosmology*, Phys. Rev. D **77**, 063516 (2008).
[3] A. Ijjas, P. J. Steinhardt and A. Loeb, *Inflationary paradigm in trouble after Planck2013*, Phys. Lett. B **723**, 261 (2013).
[4] A. H. Guth, D. I. Kaiser and Y. Nomura, *Inflationary paradigm after Planck 2013*, Phys. Lett. B **733**, 112 (2014).
[5] A. Linde (2014) *Inflationary Cosmology after Planck 2013*, [arXiv:1402.0526 [hep-th]].
[6] P. A. R. Ade *et al.* [Planck Collaboration], *Planck 2013*

- results. *XXII. Constraints on inflation*, Astron. Astrophys. **571**, A22 (2014).
- [7] P. A. R. Ade *et al.* (Planck Collaboration), *Planck 2015 results. XX. Constraints on inflation*, Astron. Astrophys. **594**, A20 (2016).
- [8] A. Berera, *Warm inflation*, Phys. Rev. Lett. **75**, 3218 (1995).
- [9] A. Berera, I. G. Moss and R. O. Ramos, *Warm Inflation and its Microphysical Basis*, Rept. Prog. Phys. **72**, 026901 (2009).
- [10] M. Bastero-Gil and A. Berera, *Warm inflation model building*, Int. J. Mod. Phys. A **24**, 2207 (2009).
- [11] G. S. Vicente, L. A. da Silva and R. O. Ramos, *Eternal inflation in a dissipative and radiation environment: Heated demise of eternity*, Phys. Rev. D **93**, no. 6, 063509 (2016).
- [12] A. Berera, *Warm inflation at arbitrary adiabaticity: A Model, an existence proof for inflationary dynamics in quantum field theory*, Nucl. Phys. B **585** 666 (2000).
- [13] R. O. Ramos, *Fine tuning solution for hybrid inflation in dissipative chaotic dynamics*, Phys. Rev. D **64**, 123510 (2001).
- [14] A. Berera and C. Gordon, *Inflationary initial conditions consistent with causality*, Phys. Rev. D **63**, 063505 (2001).
- [15] M. Bastero-Gil, A. Berera, R. Brandenberger, I. G. Moss, R. O. Ramos and J. G. Rosa, *The role of fluctuation-dissipation dynamics in setting initial conditions for inflation*, JCAP **1801**, no. 01, 002 (2018).
- [16] H. P. de Oliveira and R. O. Ramos, *Dynamical system analysis for inflation with dissipation*, Phys. Rev. D **57**, 741 (1998).
- [17] R. O. Ramos and L. A. da Silva, *Power spectrum for inflation models with quantum and thermal noises*, JCAP **1303**, 032 (2013).
- [18] S. Bartrum, M. Bastero-Gil, A. Berera, R. Cerezo, R. O. Ramos and J. G. Rosa, *The importance of being warm (during inflation)*, Phys. Lett. B **732**, 116 (2014).
- [19] M. Bastero-Gil, A. Berera, I. G. Moss and R. O. Ramos, *Cosmological fluctuations of a random field and radiation fluid*, JCAP **1405**, 004 (2014).
- [20] G. Panotopoulos and N. Videla, *Warm $\frac{\lambda}{4}\phi^4$ inflationary universe model in light of Planck 2015 results*, Eur. Phys. J. C **75**, no. 11, 525 (2015).
- [21] L. Visinelli, *Observational Constraints on Monomial Warm Inflation*, JCAP **1607**, no. 07, 054 (2016).
- [22] M. Benetti and R. O. Ramos, *Warm inflation dissipative effects: predictions and constraints from the Planck data*, Phys. Rev. D **95**, no. 2, 023517 (2017).
- [23] N. Bodendorfer (2016) *An elementary introduction to loop quantum gravity*, [arXiv:1607.05129 [gr-qc]].
- [24] D. W. Chiou, *Loop Quantum Gravity*, Int. J. Mod. Phys. D **24**, no. 01, 1530005 (2014).
- [25] A. Ashtekar and P. Singh, *Loop Quantum Cosmology: A Status Report*, Class. Quant. Grav. **28**, 213001 (2011).
- [26] A. Barrau, T. Cailleteau, J. Grain and J. Mielczarek, *Observational issues in loop quantum cosmology*, Class. Quant. Grav. **31**, 053001 (2014).
- [27] I. Agullo and P. Singh (2016) *Loop Quantum Cosmology*, [arXiv:1612.01236 [gr-qc]].
- [28] A. Ashtekar, T. Pawłowski and P. Singh, *Quantum nature of the big bang*, Phys. Rev. Lett. **96**, 141301 (2006).
- [29] A. Ashtekar, T. Pawłowski and P. Singh, *Quantum Nature of the Big Bang: Improved dynamics*, Phys. Rev. D **74**, 084003 (2006).
- [30] A. Ashtekar, A. Corichi and P. Singh, *Robustness of key features of loop quantum cosmology*, Phys. Rev. D **77**, 024046 (2008).
- [31] A. Ashtekar and D. Sloan, *Loop quantum cosmology and slow roll inflation*, Phys. Lett. B **694**, 108 (2011).
- [32] A. Ashtekar and D. Sloan, *Probability of Inflation in Loop Quantum Cosmology*, Gen. Rel. Grav. **43**, 3619 (2011).
- [33] L. Chen and J. Y. Zhu, *Loop quantum cosmology: The horizon problem and the probability of inflation*, Phys. Rev. D **92**, no. 8, 084063 (2015).
- [34] A. Corichi and A. Karami, *On the measure problem in slow roll inflation and loop quantum cosmology*, Phys. Rev. D **83**, 104006 (2011).
- [35] L. Linsefors and A. Barrau, *Duration of inflation and conditions at the bounce as a prediction of effective isotropic loop quantum cosmology*, Phys. Rev. D **87**, no. 12, 123509 (2013).
- [36] B. Bolliet, A. Barrau, K. Martineau and F. Moulin, *Some Clarifications on the Duration of Inflation in Loop Quantum Cosmology*, Class. Quant. Grav. **34**, no. 14, 145003 (2017).
- [37] M. Bastero-Gil, A. Berera, R. O. Ramos and J. G. Rosa, *Warm Little Inflaton*, Phys. Rev. Lett. **117**, no. 15, 151301 (2016).
- [38] R. Herrera, *Warm inflationary model in loop quantum cosmology*, Phys. Rev. D **81**, 123511 (2010).
- [39] K. Xiao and J. Y. Zhu, *A Phenomenology analysis of the tachyon warm inflation in loop quantum cosmology*, Phys. Lett. B **699**, 217 (2011).
- [40] X. M. Zhang and J. Y. Zhu, *Warm inflation in loop quantum cosmology: a model with a general dissipative coefficient*, Phys. Rev. D **87**, no. 4, 043522 (2013).
- [41] R. Herrera, M. Olivares and N. Videla, *General dissipative coefficient in warm intermediate inflation in loop quantum cosmology in light of Planck and BICEP2*, Int. J. Mod. Phys. D **23**, no. 10, 1450080 (2014).
- [42] S. Basilakos, V. Kamali and A. Mehrabi, *Measuring the effects of Loop Quantum Cosmology in the CMB data*, Int. J. Mod. Phys. D **26**, no. 12, 1743023 (2017).
- [43] A. Jawad, N. Videla and F. Gulshan, *Dynamics of warm power-law plateau inflation with a generalized inflaton decay rate: predictions and constraints after Planck 2015*, Eur. Phys. J. C **77**, no. 5, 271 (2017).
- [44] V. Kamali, S. Basilakos, A. Mehrabi, Meysam Motaharfard and E. Massaeli, *Tachyon warm inflation with the effects of Loop Quantum Cosmology in the light of Planck 2015*, Int. J. Mod. Phys. D **27**, no. 05, 1850056 (2018).
- [45] K. A. Meissner, *Black hole entropy in loop quantum gravity*, Class. Quant. Grav. **21**, 5245 (2004).
- [46] M. Bastero-Gil, A. Berera and R. O. Ramos, *Dissipation coefficients from scalar and fermion quantum field interactions*, JCAP **1109**, 033 (2011).
- [47] A. Berera and R. O. Ramos, *Construction of a robust warm inflation mechanism*, Phys. Lett. B **567**, 294 (2003).
- [48] M. Bastero-Gil, A. Berera, R. O. Ramos and J. G. Rosa, *General dissipation coefficient in low-temperature warm inflation*, JCAP **1301**, 016 (2013).
- [49] L. M. H. Hall, I. G. Moss and A. Berera, *Scalar perturbation spectra from warm inflation*, Phys. Rev. D **69**, 083525 (2004).
- [50] C. Graham and I. G. Moss, *Density fluctuations from warm inflation*, JCAP **07** 013 (2009).

- [51] M. Bastero-Gil, A. Berera and R. O. Ramos, *Shear viscous effects on the primordial power spectrum from warm inflation*, JCAP **07** 030 (2011).
- [52] M. Bastero-Gil, A. Berera, I. G. Moss and R. O. Ramos, *Theory of non-Gaussianity in warm inflation*, JCAP **12** 008 (2014).
- [53] L. Visinelli, *Cosmological perturbations for an inflaton field coupled to radiation*, JCAP **1501**, no. 01, 005 (2015).
- [54] M. Bastero-Gil, A. Berera, R. O. Ramos and J. G. Rosa, *Adiabatic out-of-equilibrium solutions to the Boltzmann equation in warm inflation*, JHEP **1802**, 063 (2018).
- [55] X. B. Li, H. Wang and J. Y. Zhu, *Gravitational waves from warm inflation*, Phys. Rev. D **97**, no. 6, 063516 (2018).
- [56] M. Bastero-Gil, S. Bhattacharya, K. Dutta and M. R. Gangopadhyay, *Constraining Warm Inflation with CMB data*, JCAP **1802**, no. 02, 054 (2018).
- [57] R. Arya, A. Dasgupta, G. Goswami, J. Prasad and R. Rangarajan, *Revisiting CMB constraints on warm inflation*, JCAP **1802**, no. 02, 043 (2018).
- [58] L. Parker, *Particle creation in expanding universes*, Phys. Rev. Lett. **21**, 562 (1968); L. Parker, *Quantized fields and particle creation in expanding universes. 1.*, Phys. Rev. **183**, 1057 (1969).
- [59] I. Agullo et al, *The pre-inflationary dynamics of loop quantum cosmology: Confronting quantum gravity with observations*, Class. Quantum Grav. **30**, 085014 (2013).
- [60] T. Zhu, A. Wang, G. Cleaver, K. Kirsten and Q. Sheng, *Pre-inflationary universe in loop quantum cosmology*, Phys. Rev. D **96**, no. 8, 083520 (2017).
- [61] R. Brandenberger, Q. Liang, R. O. Ramos and S. Zhou, *Fluctuations through a Vibrating Bounce*, Phys. Rev. D **97**, no. 4, 043504 (2018).
- [62] E. Wilson-Ewing, *Testing loop quantum cosmology*, Comptes Rendus Physique **18**, 207 (2017).
- [63] Y. F. Cai and E. Wilson-Ewing, *A Λ CDM bounce scenario*, JCAP **1503**, no. 03, 006 (2015).